Metallocyclodextrins as Building Blocks in Noncovalent Assemblies of Photoactive Units for the Study of Photoinduced Intercomponent Processes

Johanna M. Haider,[†] Murielle Chavarot,[†] Steffen Weidner,[†] Ian Sadler,[‡] René M. Williams,[§] Luisa De Cola,*[,§] and Zoe Pikramenou*[,†]

School of Chemistry, The University of Birmingham, Edgbaston, Birmingham B15 2TT, U.K., Department of Chemistry, The University of Edinburgh, Kings Buildings, Edinburgh, EH9 3JJ, U.K., and Molecular Photonic Materials, Institute of Molecular Chemistry, Faculty of Science, University of Amsterdam, Nieuwe Achtergracht 166, 1018 WS Amsterdam, The Netherlands

Received January 3, 2001

Cyclodextrin cups have been employed to build supramolecular systems consisting of metal and organic photoactive/redox-active components; the photoinduced communication between redox-active units assembled in water via noncovalent interactions is established. The functionalization of a β-cyclodextrin with a terpyridine unit, ttp-β-CD, is achieved by protection of all but one of the hydroxyl groups by methylation and attachment of the ttp unit on the free primary hydroxyl group. The metalloreceptors [(β-CD−ttp)Ru(ttp)][PF_6]$_2$, [(β-CD−ttp)Ru(tpy)][PF_6]$_2$, and [Ru(β-CD−ttp)$_2$][PF_6]$_2$ are synthesized and fully characterized. The [(β-CD−ttp)Ru(ttp)][PF_6]$_2$ metalloreceptor exhibits luminescence in water, centered at 640 nm, from the ^{3}MLCT state with a lifetime of 1.9 ns and a quantum yield of $\Phi = 4.1 \times 10^{-5}$. Addition of redox-active quinone guests AQS, AQC, and BQ to an aqueous solution of [(β-CD−ttp)Ru(ttp)]$^{2+}$ results in quenching of the luminescence up to 40%, 20%, and 25%, respectively. Measurement of the binding strength indicates that, in saturation conditions, 85% for AQS and 77% for AQC are bound. The luminescence quenching is attributed to an intercomponent electron transfer from the appended ruthenium center to the quinone guest inside the cavity. Control experiments demonstrate no bimolecular quenching at these conditions. A photoactive osmium metalloguest, [Os(biptpy)(tpy)][PF_6], is designed with a biphenyl hydrophobic tail for insertion in the cyclodextrin cavity. The complex is luminescent at room temperature with an emission band maximum at 730 nm and a lifetime of 116 ns. The osmium(III) species are formed for the study of photoinduced electron transfer upon their assembly with the ruthenium cyclodextrin, [(β-CD−ttp)Ru(ttp)]$^{2+}$. Time-resolved spectroscopy studies show a short component of 10 ps, attributed to electron transfer from Ru(II) to Os(III) giving an electron transfer rate 9.5×10^9 s^{-1}.

Introduction

The need for a fundamental understanding of photoinduced processes occurring in Nature has brought forth several studies involving molecular systems where the structural organization of photoactive units is dominated by noncovalent interactions.[1] From a materials perspective, efficient light-induced charge separation, as observed in natural systems, is an attractive function to generate in artificial systems for the development of photo- or optoelectronic devices.[2]

Photoactive transition metal systems have been very attractive candidates as units for the construction of molecular devices due to their photosensitization and electrochemical properties.[3] To create a long-lived charge-separated state or to funnel energy over long distances research has been mainly focused on two different approaches: (a) the attachment of organic donor and/or acceptor moieties onto ligands that coordinate to a metal center[4] and (b) the assembly of polymetallic donor/acceptor arrays. The latter approach has mainly involved the construction of covalently linked metal centers via spacer units that control the rigidity of the system or act as a relay communicator unit.[5] In such systems, high molecular complexity is inevitable as several

* E-mail: z.pikramenou@bham.ac.uk.
† The University of Birmingham.
‡ The University of Edinburgh.
§ University of Amsterdam.

(1) (a) Piotrowiak, P. *Chem. Soc. Rev.* **1999**, *28*, 143−150. (b) Kirby, J. P.; Roberts, J. A.; Nocera, D. G. *J. Am. Chem. Soc.* **1997**, *119*, 9230−9236. (c) Ward, M. D. *Chem. Soc. Rev.* **1997**, *26*, 365−375 and references herein.

(2) (a) Belser, P.; Bernhardt, S.; Blum, C.; Beyeler, A.; De Cola, L.; Balzani, V. *Coord. Chem. Rev.* **1999**, *190*−*192*, 155−159. (b) Kalyansundaram K.; Grätzel, M. *Coord. Chem. Rev.* **1998**, *177*, 347−414.

(3) (a) Balzani, V.; Juris, A.; Venturi, M.; Campagna, S.; Serroni, S. *Chem. Rev.* **1996**, *96*, 759−833. (b) Kalyanasundaram, K. *Photochemistry of Polypyridine and Porphyrin Complexes*; Academic Press: London, 1991.

(4) (a) Maxwell, K. A.; Sykora, M.; Desimone, J. M.; Meyer, T. J. *Inorg. Chem.* **2000**, *39*, 71−75. (b) Arounaguiri, S.; Maiya, B. G. *Inorg. Chem.* **1999**, *38*, 842−843. (c) Collin, J.-P.; Guillerez, S.; Sauvage, J.-P.; Barigelletti, F.; De Cola, L.; Flamigni, L.; Balzani, V. *Inorg. Chem.* **1991**, *30*, 4230−4238.

(5) (a) Barigelletti, F.; Flamigni, L. *Chem. Soc. Rev.* **2000**, *29*, 1−12. (b) El-ghayoury, A.; Harriman, A.; Khatyr, A.; Ziessel, R. *J. Phys. Chem. A* **2000**, *104*, 1512−1523. (c) Kelso, L. S.; Smith, T. A.; Schultz, A. C.; Junk, P. C.; Warrener, R. N.; Ghiggino, K. P.; Keene, F. R. *J. Chem. Soc., Dalton Trans.* **2000**, 2599−2606. (d) Constable, E. C.; Housecroft, C. E.; Schofield, E. R.; Encinas, S.; Armaroli, N.; Barigelletti, F.; Flamigni, L.; Figgemeier, E.; Vos, J. G. *Chem. Commun.* **1999**, 869−870. (e) Schlicke, B.; Belser, P.; De Cola, L.; Sabbioni, E.; Balzani, V. *J. Am. Chem. Soc.* **1999**, *121*, 4207−4214. (f) Gulyas, P. T.; Smith, T. A.; Paddon-Row, M. N. *J. Chem. Soc., Dalton Trans.* **1999**, 1325−1335. (g) Hammarström, L.; Sun, L.; Åkermark, B.; Styring, S. *Biochim. Biophys. Acta* **1998**, *1365*, 193−199. (h) De Cola, L.; Belser, P. *Coord. Chem. Rev.* **1998**, *177*, 301−346. (i) Barigelletti, F.; Flamigni, L.; Collin, J.-P.; Sauvage, J.-P. *Chem. Commun.* **1997**, 333−338.

10.1021/ic0100166 CCC: $20.00
Published on Web 07/03/2001

features are accumulated in a single molecular unit. A modular, supramolecular approach introduces a larger flexibility of choice of photoactive units. The communication of metal centers assembled via a hydrogen-bonded interface,[6] incorporated in oligonucleotides[7] or held together by a catenane structure has recently attracted attention.[8]

We are interested in employing cyclodextrins as receptors that bind guests mainly via hydrophobic interactions.[9] Our approach involves attachment of a photoactive metal to the cyclodextrin rim and assembly of another photoactive unit in close proximity via the cyclodextrin cavity to target the study of photoinduced processes between units noncovalently assembled in water. Functionalization of cyclodextrins with ligand units to attach metal centers has been widely employed, mainly for the study of enzyme mimic systems.[10] Europium and terbium luminescent cyclodextrins have been developed for sensing aromatic hydrocarbons based on an intramolecular energy transfer through the cyclodextrin cavity.[11] Ruthenium-functionalized calixarenes have also been employed in sensing schemes.[12] A porphyrin-modified cyclodextrin has been recently reported as an electron donor sensitized by a ruthenium complex in a noncovalent system designed for photoinduced electron transfer.[13] Although the synthesis of some cyclodextrins derivatized with ruthenium and rhenium bipyridine complexes had been reported,[14] these systems had not been further developed until a recent report that introduced them as sensors for the detection of steroids.[15]

We have developed several metallocyclodextrins based on transition metal photoactive units.[16] Preliminary results of one of the ruthenium−cyclodextrins showed quenching of luminescence of the appended ruthenium center upon binding of a redox-active guest. In this manuscript, we wish to report the full characterization of a terpyridine-functionalized cyclodextrin and its ruthenium−cyclodextrin complexes as well as the photophysical studies of these metallocyclodextrins with organic guests and metalloguests. The influence of three different quinones on the quenching of the ruthenium-centered luminescence was studied. Quenching is attributed to an intercomponent electron transfer process between the appended metal center and the guest included in the cavity. To extend our approach to communication of metal centers, an osmium guest with a hydrophobic tail was designed that can act as an energy (Os^{II}) as well as an electron acceptor (Os^{III}). Photoinduced electron transfer between the ruthenium(II) and osmium(III) photoactive centers assembled by the cyclodextrin cavity is demonstrated by time-resolved spectroscopy.

Experimental Section

Materials. All starting materials were purchased from Aldrich unless otherwise indicated. *β*-Cyclodextrin provided by American Maize-Products company was recrystallized from water and dried under vacuum at 80 °C for at least 6 h prior to use. Ruthenium and osmium starting materials ($RuCl_3 \cdot 3H_2O$ and OsO_4) were supplied by Johnson & Matthey. 4′-(*p*-Tolyl)-2,2′:6′,2″-terpyridine[17] (ttp), 4′-(4-biphenyl)-2,2′:6′,2″-terpyridine (biptpy),[18] $Ru(ttp)Cl_3$,[19] $Ru(tpy)Cl_3$[19] (tpy = 2,2′:6′,2″-terpyridine), $Os(tpy)Cl_3$,[20] and $[Os(tpy)(OH_2)_6][PF_6]_3$[21] were prepared according to described procedures. Solvents used in synthetic procedures were analytical grade with the exception of HPLC grade solvents used in size exclusion chromatography and spectroscopic studies. Doubly deionized water was used where necessary in the spectroscopic studies. THF was freshly distilled from sodium under nitrogen. All of the ligand synthetic procedures were carried out under nitrogen atmosphere. Thin layer chromatography (TLC) analyses were performed on either Merck silica gel 60 glass plates or Merck alumina Brockman I grade, as indicated. Biobeads SX3 was used as a stationary phase for size exclusion chromatography. Cyclodextrins were detected by an oxidizing solution consisted of anisaldehyde/acetic acid/methanol/sulfuric acid in a 2:45:430:22 ratio, following heating at around 100 °C.

Spectroscopy. NMR spectra were recorded on Bruker DRX 360 and Varian Inova 600 spectrometers. The protons on the glucose units are indicated as H_{Glu} in the assignments. Fast atom bombardment mass spectrometry was performed on a Kratos MS-50 spectrometer and electrospray on a Quattro instrument at the EPSRC Mass Spectrometry Service Centre in Swansea. Absorption spectra were recorded on a Perkin-Elmer Lambda 16 UV/vis spectrometer. Emission spectra were recorded on a Photon Technology International QM-1 steady state spectrometer described elsewhere[18] employed with a dual-grating 500/750 nm emission monochromator and appropriate cutoff filters. The spectra were not corrected for PMT response. Time-resolved emission and transient absorption spectra were obtained with a gated optical multichannel analyzer (OMA IV) of EG&G instruments similar to the ones described previously.[22] As excitation and white probe sources, a tunable Coherent Infinity laser (1 ns pulses fwhm) and an EG&G Xe flash lamp (X 504) were used, respectively. The excitation beam is at a right angle to the probing beam. The probing path length is 1 cm. Samples were adjusted to an absorption of between 0.5 and 1 (1 cm) at the excitation wavelength. Laser power was ca. 10 mJ per pulse (0.2 cm^2). Luminescence lifetimes were measured with time-correlated single photon counting using a Hamamatsu microchannel plate (R 3809) detector in a setup slightly modified from that previously described,[23] employing a frequency-doubled DCM dye laser which is synchronously pumped with a mode-locked Argon ion laser resulting in 324 nm 20 ps fwhm pulses. Decays were analyzed with a home-written deconvolution program.Quantum yields were determined using the "optical dilute relative method".[24]

Luminescence Studies. The quinone guests examined in this study were commercially available (AQS = anthraquinone-2-sulfonic acid,

(6) (a) Ghaddar, T. H.; Castner, E. W.; Isied, S. S. *J. Am. Chem. Soc.* **2000**, *122*, 1233−1234. (b) Armaroli, N.; Barigelletti, F.; Calogero, G.; Flamigni, L.; White, C. M.; Ward, M. D. *Chem. Commun.* **1997**, 2181−2182. (c) Constable, E. C.; Fallahpour, R. A. *J. Chem. Soc., Dalton Trans.* **1996**, 2389−2390.

(7) Hurley D. J.; Tor, Y. *J. Am. Chem. Soc.* **1998**, *120*, 2194−2195.

(8) Cárdenas, D. J.; Collin, J.-P.; Gaviña, P.; Sauvage, J.-P.; De Cian, A.; Fischer, J.; Armaroli, N.; Flamigni, L.; Vicinelli, V.; Balzani, V. *J. Am. Chem. Soc.* **1999**, *121*, 5481−5488.

(9) Szejtli, J. *Chem. Rev.* **1998**, *98*, 1977−1996.

(10) (a) Rizzarelli, E.; Vecchio, G. *Coord. Chem. Rev.* **1999**, *188*, 343−364. (b) Zhang, B.; Breslow, R. *J. Am. Chem. Soc.* **1997**, *119*, 1676−1681.

(11) (a) Rudzinski, C. M.; Engebretson, D. S.; Hartmann, W. K.; Nocera, D. G. *J. Phys. Chem. A* **1998**, *102*, 7442−7446. (b) Pikramenou, Z.; Yu, J.-a.; Lessard, R. B.; Ponce, A.; Wong, P. A.; Nocera, D. G. *Coord. Chem. Rev.* **1994**, *132*, 181−194.

(12) Beer, P. D.; Timoshenko, V.; Maestri, M.; Passaniti, P.; Balzani, V. *Chem. Commun.* **1999**, 1755−1756.

(13) Hamachi, I.; Takashima, H.; Hu, Y.-Z.; Shinkai, S.; Oishi, S. *Chem. Commun.* **2000**, 1127−1128.

(14) (a) Deschenaux, R.; Ruch, T.; Deschenaux, P. F.; Juris, A.; Ziessel, R. *Helv. Chim. Acta* **1995**, *78*, 619−628. (b) Deschenaux, R.; Harding, M. M.; Ruch, T. *J. Chem. Soc., Perkin Trans. 2* **1993**, 1251−1258.

(15) Nelissen, H. F. M.; Schut, A. F. J.; Venema, F.; Feiters, M. C.; Nolte, R. J. M. *Chem. Commun.* **2000**, 577−578.

(16) (a) Haider, J. M.; Pikramenou, Z. *Eur. J. Inorg. Chem.* **2001**, 189−194. (b) Chavarot M.; Pikramenou, Z. *Tetrahedron Lett.* **1999**, *40*, 6865−6868. (c) Weidner, S.; Pikramenou, Z. *Chem. Commun.* **1998**, 1473−1474.

(17) Kröhnke, F. *Synthesis* **1976**, 1−24.

(18) Alcock, N. W.; Barker, P. R.; Haider, J. M.; Hannon, M. J.; Painting, C. L.; Pikramenou, Z.; Plummer, E. A.; Rissanen, K.; Saarenketo, P. *J. Chem. Soc., Dalton Trans.* **2000**, 1447−1461.

(19) Sullivan, B. P.; Calvert, J. M.; Meyer, T. J. *Inorg. Chem.* **1980**, *19*, 1404−1407.

(20) Buckingham, D. A.; Dwyer, F. P.; Sargeson, A. M. *Aust. J. Chem.* **1961**, *14*, 250−258.

(21) Vogler L. M.; Brewer, K. J. *Inorg. Chem.* **1996**, *35*, 818−824.

(22) Vanstokkum, I. H. M.; Scherer, T.; Brouwer, A. M.; Verhoeven, J. W. *J. Phys. Chem.* **1994**, *98*, 852−866.

(23) Bebelaar D. *Rev. Sci. Instrum.* **1986**, *57*, 1116−1125.

(24) Demas, J. N.; Crosby, G. A. *J. Phys. Chem.* **1971**, *75*, 991−1024.

AQC = anthraquinone-2-carboxylic acid, BQ = 1,4-benzoquinone) and recrystallized prior to use. The quinone quenching experiments were performed in buffered solutions (BDH 50 mM phosphate buffer, pH = 7). Stock solutions of the quinones were prepared in the buffer (AQS and BQ) or acetonitrile (AQC). Microliter quantities of the quinone stock solution were added to a $[Ru(ttp)(ttp\text{-}\beta\text{-}CD)][PF_6]_2$ (2.83×10^{-5} M) solution. Guest concentrations ranged from 1.11×10^{-4} to 4.17×10^{-3} M for AQS, from 3.91×10^{-5} to 1.47×10^{-3} M for AQC, and from 6.13×10^{-4} to 2.64×10^{-2} M for BQ. Corrections of the dilution effects were performed where necessary. The area of the ruthenium emission signal was integrated upon each addition of the guest. The control experiments were performed in acetonitrile under the same conditions using $[Ru(ttp)_2][PF_6]_2$ as a model ruthenium compound without a recognition site in place of the ruthenium−cyclodextrin.

The transient absorption spectroscopy experiments with AQC as a guest were performed in conditions similar to those used for the steady state emission experiments ($[Ru(ttp)(ttp\text{-}\beta\text{-}CD)(PF_6)_2] = 1.26 \times 10^{-4}$ M and [AQS] ranged from 7.18×10^{-4} to 2.86×10^{-3} M).

In the case of the osmium metalloguest the experiments were performed in aqueous solution with 10% CH_3CN as optimum conditions for binding and solubility. In the steady state luminescence experiments, excess $[Ru(ttp)(ttp\text{-}\beta\text{-}CD)][PF_6]_2$ was used (ranged from 9.1×10^{-6} to 3.03×10^{-5} M) in a solution of $[Os^{II}(biptpy)(tpy)][PF_6]_2$ (2.6×10^{-6} M). The area of the osmium emission signal was integrated, after excitation at 490 and 662 nm. For each excess of the host, an isoabsorptive solution of $[Os^{II}(biptpy)(tpy)][PF_6]_2$ was prepared (from 1.16×10^{-5} to 4.25×10^{-5} M) and the osmium emission signal was integrated. The different integrations were compared, by calculating the ratios I^{490}/I^{490}_{iso} and I^{662}/I^{662}_{iso}. In the time-resolved experiments excess $[Os^{II}(biptpy)(tpy)][PF_6]_2$ was added (2.35×10^{-4} M) to $[Ru(ttp)(ttp\text{-}\beta\text{-}CD)][PF_6]_2$ at a concentration of 3.15×10^{-5} M. The Os(III) complex was generated in situ by addition of an equimolar amount of $(NH_4)_4Ce(SO_4)_4$ in 6% HNO_3 to the solution used in the aforementioned study following a procedure described previously.[25]

Binding Studies. The assembly of the guests in the cyclodextrins was independently examined by monitoring the intrinsic luminescence properties of the guests.[26] Permethylated β-cyclodextrin was used as a model compound with no interfering UV−vis absorption bands for the study of guest inclusion properties. Luminescence properties of the guest molecules change upon inclusion in the cyclodextrin cavity due to a more nonpolar and sterically restricted environment. A 70 W Xe lamp was employed for the excitation of quinones to avoid their decomposition under long UV exposure. The binding studies were performed in buffer solutions as the ruthenium-quenching experiments. Microliter quantities of a concentrated solution of cyclodextrin were added to the respective quinone solution ([AQS] = 1.02×10^{-4} M and [AQC] = 1.72×10^{-4} M). Excess the cyclodextrin was attained in each case: 7−100 times excess (7.07×10^{-4} to 1.06×10^{-2} M) in the AQS case, and 7−77 times excess in AQC solution (1.28×10^{-3} to 1.32×10^{-2} M). Following each addition the solution was stirred for 8 min to ensure equilibration. The data of the emission signal were obtained by integration of the signal in the area of 360−752 nm and interpreted by nonlinear least-squares fitting methods to yield binding constant values, K_a, for a 1:1 equilibrium between the host and the guest molecule. We estimated binding constants of 860 ± 200 and 1100 ± 100 M^{-1} for the inclusion of AQC and AQS, respectively, in permethylated β-cyclodextrin. BQ binding was not examined by this method due to the instability of the compound under UV excitation. However, a binding constant of around 100 M^{-1} for BQ binding can be calculated from the quenching experiments of the ruthenium−cyclodextrins. Excess quinones were used in the quenching experiments of the ruthenium−cyclodextrin luminescence to ensure that most of the guest was bound (in saturation conditions 85% for AQS and 77% for AQC). The binding of metalloguests was estimated by inclusion studies of biptpy in permethylated β-cyclodextrin.[27] In the case of the biphenyl−terpyridine an association of $2 \times 10^4 \pm 1 \times 10^3$ M^{-1} has been estimated.

Synthesis. 4′-(*p*-(Bromomethyl)phenyl)-2,2′:6′,2″-terpyridine (ttp-CH_2Br).[28] A solution of 4′-(*p*-tolyl)-2,2′:6′,2″-terpyridine (0.65 g, 2.01 mmol), *N*-bromosuccinimide (0.37 g, 2.07 mmol), and dibenzoyl peroxide was left to reflux in 120 mL of carbon tetrachloride for 6 h. TLC analysis (Al_2O_3; diethyl ether/hexane 1:1) indicated that only 4′-(*p*-(bromomethyl)phenyl)-2,2′:6′,2″-terpyridine ($R_f = 0.40$) was formed. The yellow brown mixture was allowed to cool down to room temperature, filtered, washed with 2 × 10 mL of water, and dried over anhydrous Na_2SO_4. The solvent was evaporated, and the residue was recrystallized from a 2:1 ethanol/acetone solvent mixture to yield the pure 4′-(*p*-(bromomethyl)phenyl)-2,2′:6′,2″-terpyridine as a solid (0.46 g, yield: 57%).

^{1}H NMR (250 MHz, $CDCl_3$): δ in ppm 8.72 (s, 2H, H-3′), 8.66 (d, $J = 8.0$ Hz, 4H, H-3 and H-6), 7.92−7.83 (m, 4H, H-4 and H*o*), 7.52 (d, $J = 8.2$ Hz, 2H, H*m*), 7.38−7.32 (m, 2H, H-5), 4.56 (s, 2H, $-CH_2$-Br).

FAB-MS (NOBA matrix): *m*/*z* 402 $\{M + H\}^+$.

Mono-6-hydroxy Permethylated β-Cyclodextrin (β-CD−OH). The synthetic procedure of Bradshaw et al. was followed.[29] Purification was performed by flash chromatography, using a Biotage prepacked silica column (eluent system, ethyl acetate/methanol, 10:0.5; eluent system for TLC, ethyl acetate/methanol, 9:1), yielding mono-6-hydroxy permethylated β-cyclodextrin (yield: 25%, $R_{f(TLC)} = 0.19$) and permethylated β-cyclodextrin (yield: 16%, $R_{f(TLC)} = 0.31$). Characterization of the compound by NMR spectroscopy and mass spectrometry agrees with the previously published data. Selective data are given below.

^{1}H NMR (360 MHz, $CDCl_3$): δ in ppm 5.22 (d, $J = 3.6$ Hz, 1H, H_{Glu}-1), 5.15 (dd, 2H, H_{Glu}-1), 5.09 (d, $J = 3.6$ Hz, 3H, H_{Glu}-1), 5.02 (d, $J = 3.6$ Hz, 1H, H_{Glu}-1), 3.92−3.69 (m, H_{Glu}-5,6), 3.6−3.3, (m, H_{Glu}-3,4,6′-OCH_3), 3.22 (m, H_{Glu}-2).

ES-MS (MeOH): *m*/*z* 1438 $\{M + Na\}^+$, 730 $\{M + 2Na\}^{2+}$.

Anal. Found: C, 51.7; H, 7.7. Calcd for $C_{62}H_{110}O_{35}\cdot 1H_2O$: C, 51.9; H, 7.9.

β-CD−ttp. To a solution of β-CD−OH (382 mg, 0.27 mmol) in 10 mL of dry THF cooled to 0 °C, sodium hydride (65 mg, 2.7 mmol) was added with vigorous stirring. When addition was complete, the mixture was allowed to warm up to room temperature and was kept at 50−55 °C for 1 h. ttp-CH_2Br (143 mg, 0.36 mmol) dissolved in 15 mL of THF was added at room temperature, and the solution was brought to reflux for 24 h. The reaction was followed by TLC (Al_2O_3; ethyl acetate/methanol, 10:0.1, R_f: product = 0.54, mono-6-hydroxy permethylated β-cyclodextrin = 0.22 and ttp-CH_2Br = 0.96, respectively). The reaction mixture was then hydrolyzed with a saturated aqueous solution of NaCl at 0 °C. Following evaporation of the THF, the aqueous phase was extracted with dichloromethane (4 × 50 mL). The combined organic phases were dried over Na_2SO_4, filtered, and concentrated. The solid obtained was purified by chromatography on alumina gel by using a mixture of ethyl acetate/ethanol, 10:0.1, as eluent (330 mg, yield: 71%).

^{1}H NMR (600 MHz, $CDCl_3$): δ in ppm 8.73−8.72 (m, 4H, H-3′ and H-6), 8.66 (d, $J = 7.9$ Hz, 2H, H-3), 7.89 (d, $J = 7.3$ Hz, 2H, H*m*), 7.87 (m, 2H, H-4), 7.48 (d, $J = 7.2$ Hz, 2H, H*o*), 7.35 (m, 2H, H-5), 5.13−5.06 (m, 7H, H_{Glu}-1), 4.70 (d, $J = 12.5$ Hz, 1H, $-CH_2$-benzyl), 4.64 (d, $J = 12.5$ Hz, 1H, $-CH_2$-benzyl), 3.99 (dd, $J = 10.6$ and 4.0 Hz, 1H, H_{Glu}-6), 4.0−3.0 (m, $-OCH_3$ and H_{Glu}-2,3,4,5,6).

FAB-MS (NOBA matrix): *m*/*z* 1738 $\{M + H\}^+$.

Anal. Found: C, 56.4; H, 7.4; N, 2.2. Calcd for $C_{84}H_{125}N_3O_{35}\cdot 3H_2O$: C, 56.3; H, 7.4; N, 2.3.

Ru(β-CD−ttp)Cl_3. β-CD−ttp (90 mg 0.052 mmol) was added to a solution of $RuCl_3\cdot 3H_2O$ (13.6 mg, 0.052 mmol) in 15 mL of absolute ethanol. The mixture was heated at reflux for 4 h while vigorous magnetic stirring was maintained. The mixture was allowed to cool to room temperature, extracted with dichloromethane, and dried over

(25) De Cola, L.; Balzani, V.; Barigelletti, F.; Flamigni, L.; Belser, P.; von Zelewsky, A.; Franck, M.; Vögtle, F. *Inorg. Chem.* **1993**, *32*, 5228−5238.

(26) Davis, J. E. D.; Ripmeester, J. A. In *Comprehensive Supramolecular Chemistry*; Atwood, J. L., Davies, J. E. D., MacNicol, D. D., Vögtle, F., Eds.; Pergamon: Oxford, 1996; Vol. 8.

(27) Haider, J. M.; Pikramenou, Z. Manuscript in preparation.

(28) Collin, J.-P.; Guillerez, S.; Sauvage, J.-P.; Barigelletti, F.; De Cola, L.; Flamigni, L.; Balzani, V. *Inorg. Chem.* **1991**, *30*, 4230−4238.

(29) Chen, Z.; Bradshaw, J. S.; Lee, M. L. *Tetrahedron Lett.* **1996**, *37* (38), 6831−6834.

$MgSO_4$ and the solvent was evaporated. The reaction gave 86 mg of Ru(β-CD−ttp)Cl_3 (yield: 85%).

FAB-MS (DMSO/3-NOBA matrix): *m*/*z* 1945 $\{M + H\}^+$.

[(β-CD−ttp)Ru(ttp)][PF_6]$_2$. A mixture of β-CD−ttp (90 mg, 0.052 mmol), Ru(ttp)Cl_3 (13.6 mg, 0.052 mmol), and a few drops of *N*-ethylmorpholine in 7 mL of methanol was left to reflux for 24 h. After cooling to room temperature, the mixture was filtered through Celite and a methanolic solution of ammonium hexafluorophosphate (20 mg, 0.123 mmol) was added to the dark red filtrate. The compound was extracted with dichloromethane and purified by size exclusion chromatography (BioBeads SX3; DMF/THF 1:1) (92 mg, yield: 58%).

^{1}H NMR (600 MHz, $CDCl_3$): δ in ppm 8.78 (s, 2H, H-3′), 8.77 (s, 2H, H_{ttp}-3′), 8.48 (d, J = 8.0 Hz, 4H, H-3 and H_{ttp}-3), 8.08 (d, J = 8.1 Hz, 2H, H*m*), 8.00 (d, J = 8.0 Hz, 2H, H_{ttp}-*m*), 7.79 (m, 4H, H-4 and H_{ttp}-4), 7.64 (d, J = 8.1 Hz, 2H, H*o*), 7.40 (d, J = 8.0 Hz, 2H, H_{ttp}-*o*), 7.35 (m, 4H, H-6 and H_{ttp}-6), 7.15 (m, 4H, H-5 and H_{ttp}-5), 5.22−5.08 (m, 7H, H_{Glu}-1), 4.74 (d, J = 13.9 Hz, 1H, −CH_2-benzyl), 4.73 (d, J = 13.9 Hz, 1H, −CH_2-benzyl), 4.15 (dd, J = 10.8 and 3.2 Hz, 1H, H_{Glu}-6), 3.9−3.16 (m, −OCH_3 and H_{Glu}-2,3,4,5,6).

FAB-MS (NOBA matrix): *m*/*z* 2161 $\{M - [PF_6]\}^+$, 2306 $\{M - 2[PF_6]\}^{2+}$, 2451 M^+.

UV−vis in CH_3CN: λ_{max} in nm (ϵ in M^{-1} cm^{-1}) 490 (28600), 310 (77600) 282 (72400). In H_2O: λ_{max} in nm (ϵ in M^{-1} cm^{-1}) 490 (26000), 310 (60100) 282 (58258).

Anal. Found: C, 51.7; H, 6.1; N, 3.3. Calcd for $C_{106}H_{142}N_6O_{35}P_2F_6$-Ru: C, 51.9; H, 5.8; N, 3.4.

[(β-CD−ttp)Ru(tpy)][PF_6]$_2$. A similar procedure as for [(β-CD−ttp)Ru(ttp)][PF_6]$_2$ was followed using Ru(tpy)Cl_3 and β-CD−ttp. Yield: 79%.

^{1}H NMR (600 MHz, $CDCl_3$): δ in ppm 8.78 (s, 3H, H-3′), 8.64 (d, J = 8.2 Hz, 2H, H_{tpy}-3′), 8.49 (d, J = 8.2 Hz, 2H, H-3), 8.67 (d, J = 7.2 Hz, 2H, H_{tpy}-3), 8.09 (d, J = 8.1 Hz, 2H, H*m*), 7.83 (m, 2H, H-4), 7.79 (m, 2H, H_{tpy}-4), 7.67 (d, J = 8.1 Hz, 2H, H*o*), 7.39 (d, J = 5.1 Hz, 2H, H-6), 7.35 (d, J = 5.2 Hz, 2H, H_{tpy}-6), 7.29 (m, 1H, H_{tpy}-4′), 7.18 (m, 4H, H-5 and H_{tpy}-5), 5.22−5.08 (m, 7H, H_{Glu}-1), 4.76 (d, J = 12.8 Hz, 1H, −CH_2-benzyl), 4.74 (d, J = 12.8 Hz, 1H, −CH_2-benzyl), 4.15 (dd, J = 10.8 and 3.0 Hz, 1H, H_{Glu}-6), 3.9−3.16 (m, −OCH_3 and H_{Glu}-2,3,4,5,6).

FAB-MS (NOBA matrix): *m*/*z* 2216 $\{M - [PF_6]\}^+$, 2071 $\{M - 2[PF_6]\}^{2+}$.

UV−vis (CH_3CN): λ_{max} in nm (ϵ in M^{-1} cm^{-1}) 483 (19000), 309 (64000) 283 (45000).

[Ru(β-CD−ttp)$_2$][PF_6]$_2$. A mixture of β-CD−ttp (45 mg, 0.026 mmol), Ru(β-CD−ttp)Cl_3 (51 mg, 0.026 mmol), and few drops of *N*-ethylmorpholine in 7 mL of methanol was brought to reflux for 24 h. After cooling to room temperature, the mixture was concentrated and a methanolic solution of ammonium hexafluorophosphate was added. The compound was extracted with dichloromethane, and the product was then purified by size exclusion chromatography (BioBeads SX3; DMF/THF 1:1) to give 65 mg of pure complex (yield: 64%).

^{1}H NMR (600 MHz, $CDCl_3$): δ in ppm 8.78 (s, 4H, H-3′), 8.50 (d, J = 7.9 Hz, 4H, H-3), 8.07 (d, J = 7.9 Hz, 4H, H*m*), 7.83 (m, 4H, H-4), 7.64 (d, J = 8.0 Hz, 4H, H*o*), 7.39 (d, J = 5.3 Hz, 4H, H-6), 7.19 (m, 4H, H-5), 5.19−5.07 (m, 14H, H_{Glu}-1), 4.73 (dd, 4H, −CH_2-benzyl), 4.12 (dd, 2H, H_{Glu}-6), 3.9−3.16 (m, −OCH_3 and H_{Glu}-2,3,4,5,6).

ESMS (CH_3CN): *m*/*z* 1788 $\{M - 2[PF_6]\}^{2+}$.

UV−vis (CH_3CN): λ_{max} in nm (ϵ in M^{-1} cm^{-1}) 490 (2.6×10^4), 311 (6.4×10^4), 285 (6.5×10^4).

[Os(biptpy)(tpy)][PF_6]$_2$. [Os(tpy)$(OH_2)_3$][PF_6]$_3$ (26 mg; 0.03 mmol) and biptpy (13.2 mg; 1.2 eq) were heated at 120 °C in 5 mL of ethylene glycol for 30 min. After subsequent cooling to room temperature, a methanolic solution of ammonium hexafluorophosphate was added, resulting in the precipitation of a brown powder, which was filtered off and washed with water. The crude compound was purified by chromatography on silica (eluent: CH_3CN/aqueous saturated solution of KNO_3, 9:1). The pure complex was precipitated by addition of a methanolic solution of NH_4PF_6, to give 26 mg (0.024 mmol, yield: 79%).

^{1}H NMR (600 MHz, CD_3OD): δ in ppm 9.32 (s, 2H, H-3′), 8.95 (d, J = 8.2 Hz, 2H, H_{tpy}-3′), 8.86 (d, J = 8.1 Hz, 2H, H-3), 8.66 (d, J = 8.0 Hz, 2H, H_{tpy}-3), 8.35 (d, J = 8.3 Hz, 2H, Ha/b), 8.00 (d, J = 8.4 Hz, 2H, Ha/b), 7.98 (t, J = 8.2 Hz, 1H, H_{tpy}-4′), 7.86 (ddd, J = 8.0, 7.9 and 1.4 Hz, 2H, H-4), 7.84 (ddd, J = 8.1, 8.0 and 1.5 Hz, 2H, H_{tpy}-4), 7.78 (d, J = 8.2 and 1.2 Hz, 2H, H*o*), 7.53 (t, J = 7.8 Hz, 2H, H*m*), 7.43 (d, J = 5.2 Hz, 2H, H_{tpy}-6), 7.41 (dd, J = 7.4 and 1.2 Hz, 1H, H*p*), 7.34 (dd, J = 5.8 and 0.7 Hz, 2H, H-6), 7.19 (ddd, J = 7.4, 6.0 and 1.3 Hz, 4H, H-5 and H_{tpy}-5).

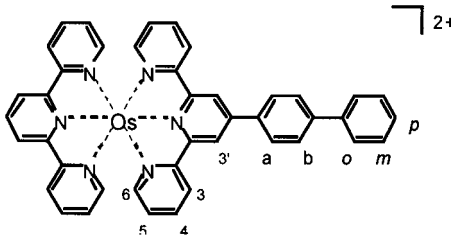

FAB-MS (NOBA matrix): *m*/*z* 810 $\{M - 2[PF_6]\}^{2+}$.

UV−vis in CH_3CN: λ_{max} in nm (ϵ in M^{-1} cm^{-1}) 662 (5125), 485 (21200). In CH_3CN/H_2O (1:9): λ_{max} in nm (ϵ in M^{-1} cm^{-1}) 662 (4820), 485 (20770).

Anal. Found: C, 44.8; H, 2.7; N, 7.4. Calcd for $C_{42}H_{30}N_6P_2F_6Os$: C, 45.9; H, 2.8; N, 7.6.

Results and Discussion

Synthesis. Cyclodextrin substitution chemistry has attracted a lot of interest for the wealth of functionalization patterns available for the primary and secondary glucose hydroxyl groups.[30] A prerequisite for our design was solubility of the metallocyclodextrins in both aqueous and organic solvent systems, in order to achieve isolation of the pure complexes by chromatographic methods as well as to perform the binding of the photoactive guest in aqueous conditions to ensure strong association. For this reason we chose to work with methylated cyclodextrins. The functionalization of the β-cyclodextrin with one metal coordinating unit was achieved by employing a cyclodextrin with only one reactive group and blocking all the rest by methylation of the hydroxy sites (Scheme 1).

Mono-6-hydroxy permethylated β-cyclodextrin (β-CD−OH)[29] fitted our design for a precursor. The attachment of a terpyridine unit was achieved using Williamson ether conditions[14b] via the bromide of 4′-(*p*-tolyl)-2,2′:6′,2″-terpyridine. The ruthenium complexes were prepared by a modification of a standard method for the synthesis of 2,2′:6′,2″-terpyridine complexes,[31] via a stepwise addition of the two terpyridines to the metal center. In the first step, the paramagnetic [Ru(tpy-X)Cl_3] [X= H, tolyl, 4-(β-cyclodextrin)tolyl] was isolated; it was then treated with *N*-ethylmorpholine, which is a mild reducing agent, and β-CD−ttp to give homoleptic [Ru(β-CD−ttp)$_2$]$^{2+}$ and heteroleptic [Ru(ttp)(β-CD−ttp)]$^{2+}$ and [Ru(tpy)(β-CD−ttp)]$^{2+}$ complexes. The metallocyclodextrins proved to be very soluble in alcoholic solution; therefore, precipitation by anion displacement was not successful and size exclusion chromatography was employed to give the pure complexes. The yields are in the same range as those for substituted terpyridine ruthenium complexes.[32]

In order to form an osmium complex that can act as a guest we designed a ligand with a hydrophobic tail to be attached to the photoactive metal center. Biphenyl-based moieties have been

(30) Khan, A. R.; Forgo, P.; Stine K. J.; D'Souza, V. T. *Chem. Rev.* **1998**, *98*, 1977−1996.
(31) Maestri, M.; Armaroli, N.; Balzani, V.; Constable, E. C.; Cargill Thompson, A. M. W. *Inorg. Chem.* **1995**, *34*, 2759−2767.
(32) Constable, E. C.; Cargill Thompson, A. M. W.; Tocher, D. A.; Daniels, M. A. M. *New J. Chem.* **1992**, *16*, 855−867.

Scheme 1

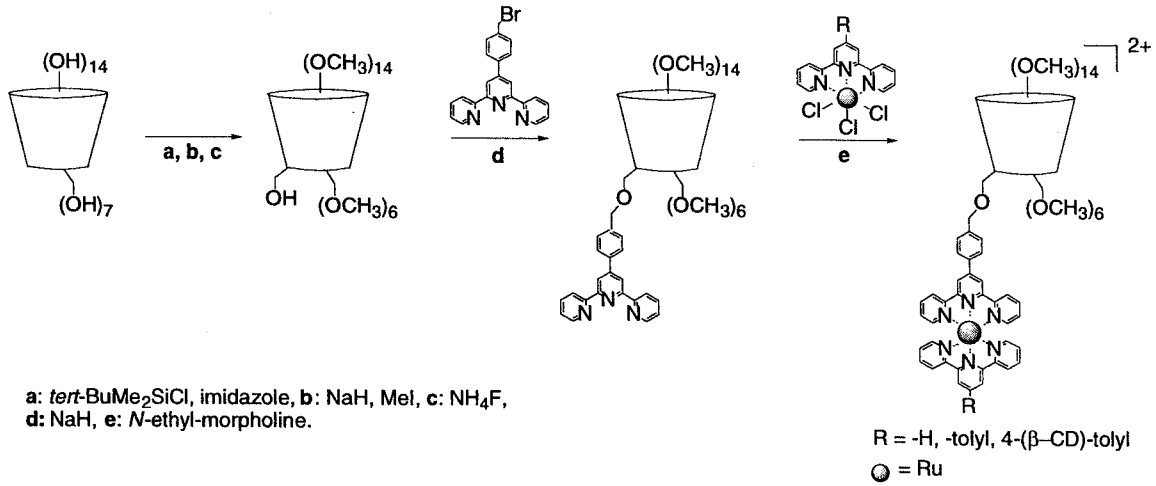

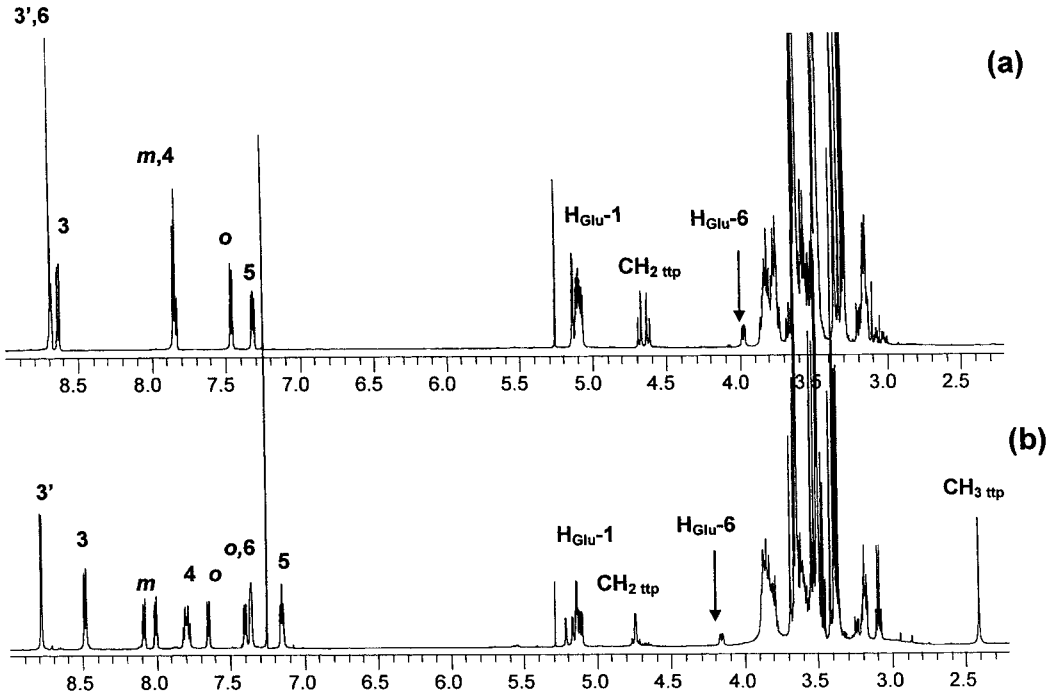

Figure 1. The 600 MHz ^{1}H NMR spectra of (a) ttp-β-CD and (b) [Ru(ttp)(ttp-β-CD)][PF_6]$_2$ in $CDCl_3$. Assignments of some protons are indicated.

reported to form inclusion complexes with cyclodextrins.[33] A 4′-(4-biphenyl)-2,2′;6′,2″-terpyridine (biptpy) ligand which was recently reported[18] and which is also easily accessible via Khrönke synthesis fitted our design. The heteroleptic complex [Os(biptpy)(tpy)][PF_6]$_2$ was prepared with a good yield, using the procedure described by Brewer et al.[21] This synthesis, starting from the commercially available osmium trichloride, avoids the formation of a mixture of homoleptic and heteroleptic complexes, by a stepwise addition of the ligands to the metal. Due to the poor reactivity of Os(tpy)Cl_3, [Os(tpy)(H_2O)$_3$][PF_6]$_3$ is used as a synthetic intermediate.

Characterization. All reported compounds have been characterized by ^{1}H NMR spectroscopy and mass spectrometry. High-field NMR methods have proven to be successful in the identification and characterization of unsymmetrical substituted cyclodextrins where the seven glucose units become nonequivalent and each glucose unit has one set of different proton resonances.[34] Due to the similarity of the seven sugar rings, there is a high degree of spectral overlap of the protons and interpretation of single resonances becomes nontrivial. We employed 1D and 2D homonuclear proton correlation (COSY, TOCSY) techniques for the identification of the ligand and the complexes.

The 1D ^{1}H NMR spectrum of the ligand β-CD−ttp shows the glucose resonances in the low-frequency and characteristic aromatic tolyl−terpyridine signals in the high-frequency part (Figure 1a).

Integration of signal intensities of the two regions gives a 1:1 signal ratio confirming monosubstitution of the cyclodextrin by the ligand unit. The methylene protons of the ttp moiety appear at 4.7 and 4.6 ppm. The original singlet of ttpCH_2Br is split into a doublet of doublets due to the chiral nature of the substituted β-CD−ttp and shifted to higher frequency compared

(33) (a) Sanemasa, I.; Wu, J. S.; Toda, K. *Bull. Chem. Soc. Jpn.* **1997**, *70*, 365−369. (b) Yamamoto, Y.; Yoshida, Y.; Tagawa, S. *Bull. Chem. Soc. Jpn.* **1996**, *69*, 2163−2166.

(34) Spencer, C. M.; Stoddart, J. F.; Zarzycki, R. *J. Chem. Soc., Perkin Trans. 2* **1987**, 1323−1336.

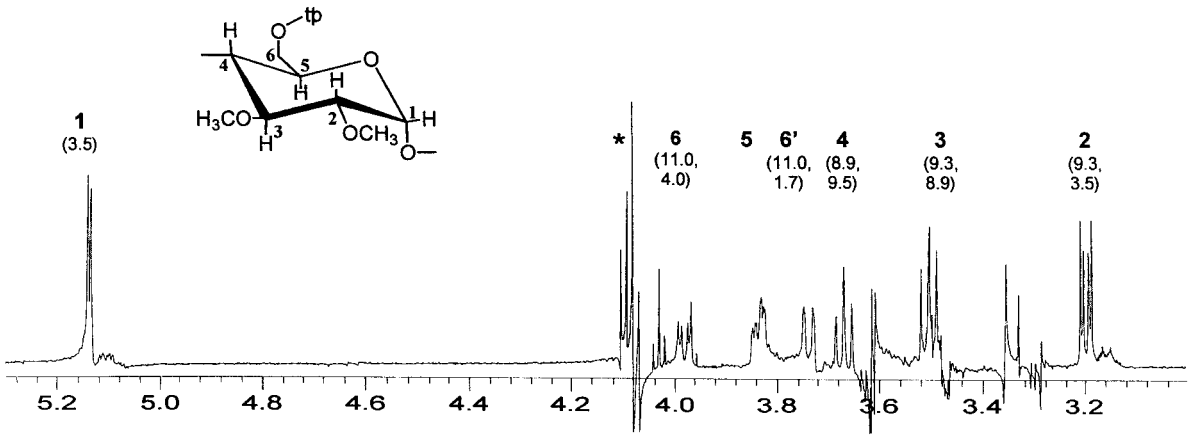

Figure 2. The 600 MHz 1D ^{1}H TOCSY spectrum of ttp-β-CD in $CDCl_3$. Only the region of the glucose protons is shown; selective excitation of an H-6 proton reveals the rest of the protons of the substituted glucose ring. An asterisk (*) indicates ethyl acetate presence in the sample; coupling constants are given in parentheses.

to the starting material confirming the replacement of the bromide with the newly formed ether bond. The shifts obtained for the aromatic region of β-CD−ttp are very similar to those of ttp, as anticipated. The H-3′ protons of the central pyridine ring appear as a singlet at a lower field, close to a doublet for the H-6 protons. The peak of the H-6 protons shows cross peaks to the multiplets at 7.4 and 7.9 ppm in COSY and TOCSY experiments, which were identified as protons on the H-5 and H-4 positions, respectively. A further cross peak with the doublet at 8.7 ppm is assigned to the H-3 position. The doublets of ortho and meta protons of the tolyl ring at 7.5 and 7.8 ppm, respectively, just show coupling to each other and were identified by their chemical shifts.

Cyclodextrin resonances of β-CD−ttp appear between 5.2 and 3.1 ppm. The seven anomeric protons are very distinctive and were found in the region of 5.1 ppm. They consist of a set of seven doublets, with the doublet at the highest frequency assigned to the substituted glucose unit. Starting from the anomeric protons, one can assign sequentially the protons in a given sugar from COSY and TOCSY experiments. H-2 signals were found in the region at 3.2 ppm, H-3 signals at 3.5 ppm, and H-4, H-5, and H-6 signals in the region from 3.6 to 3.9 ppm. The methoxy groups are shown at 3.1, 3.5, and 3.6 ppm for the 6-, 2-, and 3-methoxy groups, respectively, in agreement with previous reports.[35] Of special interest is the doublet of doublets at 4.0 ppm, which belongs to one of the two diastereotopic H_{Glu}-6 protons of the substituted glucose ring. A selected pulse on that resonance in a 1D TOCSY experiment reveals the protons of the substituted glucose ring which can be easily assigned as shown in Figure 2.

The diastereotopic H-6 and H-6′ show an 11 Hz coupling between them and two different couplings to H-5, 4.0 and 1.7 Hz, respectively. The coupling constant of 4 Hz indicates an angle between the H-6 and H-5 protons close to 90°. The rest of the proton coupling constants agree with the pattern commonly found for axial/equatorial positions in glucose rings. This suggests that the substitution has not altered the conformation of the glucose ring.

The ^{1}H NMR spectra of $[Ru(ttp)(\beta\text{-CD}-ttp)]^{2+}$ and $[Ru(tpy)(\beta\text{-CD}-ttp)]^{2+}$ can be described as the sum spectra of $[Ru(ttp)_2]^{2+}$/$[Ru(tpy)_2]^{2+}$ and $[Ru(\beta\text{-CD}-ttp)_2]^{2+}$. The $[Ru(\beta\text{-CD}-ttp)_2]^{2+}$ complex is a highly symmetric compound and shows a simple ^{1}H pattern for the aromatics. The 600 MHz ^{1}H NMR spectrum of $[Ru(ttp)(\beta\text{-CD}-ttp)]^{2+}$ (Figure 1b) revealed several shifts in comparison to the free ligand β-CD−ttp. In the aromatic part, a remarkable upfield shift of the 6-protons (−1.1 ppm) due to ruthenium complexation was observed. The rest of the shifts are consistent with those observed in previous studies[32] for complexation of terpyridine ligands with metal centers. In the aliphatic part, the two diastereotopic benzyl methylene protons are shifted downfield with a slightly higher coupling constant, indicating a conformational change upon metal complexation.

Cyclodextrin resonances are found between 5.2 and 3.2 ppm. The anomeric protons around 5.1 ppm were dispersed in a 1:1:3:1:1 ratio with the doublet of the substituted unit coming at lowest field. No changes of the coupling constant were observed upon metal complexation. The separated diastereotopic H_{Glu}-6 in the substituted glucose unit appear at lower frequency than the free ligand with a smaller coupling constant to H_{Glu}-5. For the rest of the cyclodextrin resonances, which appear between 3.9 and 3.2 ppm, only minor shifts compared to the free ligand were found.

The redox potentials of the ruthenium cyclodextrin compounds are very similar to the parent compound $[Ru(ttp)_2]^{2+}$.[36] Oxidation potentials in acetonitrile solutions (0.03 mM) were +0.83 and +0.86 V vs Fc^+/Fc, and reduction potentials are at −1.63 and −1.62 V vs Fc^+/Fc for $[Ru(ttp)(\beta\text{-CD}-ttp)]^{2+}$ and $[Ru(\beta\text{-CD}-ttp)_2]^{2+}$ (electrolyte was tetrabutylammonium hexafluorophosphate).

Luminescence Studies. Photophysical Properties of Ruthenium Cyclodextrins and Osmium Metalloguests. The ruthenium−cyclodextrin complexes showed luminescence at 640 nm from the ^{3}MLCT excited state as expected (Figure 3).

The attachment of cyclodextrin cavities at ruthenium photoactive units permits photophysical studies in both aqueous and organic solvents due to the versatile solubility properties of the methylated cyclodextrin cavity. Although the λ_{max} of the ^{3}MLCT luminescence is not significantly shifted in comparison with $Ru(ttp)_2^{2+}$, the luminescence lifetimes and quantum yield values for $[Ru(ttp)(\beta\text{-CD}-ttp)][PF_6]_2$ and $[Ru(\beta\text{-CD}-ttp)_2][PF_6]_2$ in acetonitrile are slightly higher. The luminescence quantum yield of the Ru−cyclodextrin compound $[Ru(ttp)(\beta\text{-CD}-ttp)]^{2+}$ in acetonitrile is $\Phi = 4.1 \times 10^{-5}$ whereas for the parent compound it is 3.2×10^{-5}. Also the excited state lifetime is slightly longer: $\tau = 1.9$ ns $[Ru(ttp)(\beta\text{-CD}-ttp)]^{2+}$ versus $\tau = 0.95$ ns

(35) Johnson, J. R.; Shankland, N.; Sadler, I. H. *Tetrahedron* **1985**, *41*, 3147−3152.

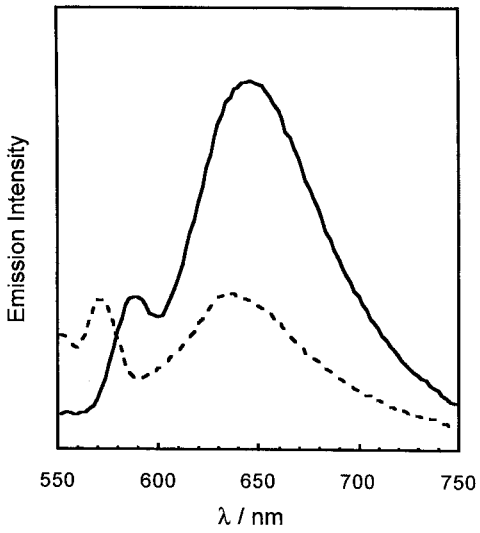

Figure 3. Luminescence spectra of $[Ru(ttp)(ttp\text{-}\beta\text{-}CD)][PF_6]_2$ in CH_3CN (dashed curve) and H_2O (solid line). The intensity is not to scale.

$[Ru(ttp)_2]^{2+}$.[36] In a previous report of a ruthenium cyclodextrin a decrease in the luminescence lifetime was observed upon comparison with the parent compound due to steric constraints involving a 6-substituted bipyridine ligand.[14a] In our case we can conclude that there is no steric hindrance to influence the luminescence properties of the units. However, it is interesting to note that due to the weak luminescence of the $Ru(ttp)_2^{2+}$ unit, Raman bands of the solvent are observed in the luminescence spectrum at 570 nm for acetonitrile and 590 nm for water (for $\lambda_{exc} = 490$ nm) that can obscure the luminescence signal in some cases.[37] We have employed the luminescent ruthenium cyclodextrins to study communication of the ruthenium center with quinone guests and metalloguest molecules included in the cyclodextrin cavity in aqueous solutions.

Osmium complexes are attractive candidates as energy acceptors in multimetallic assemblies with ruthenium-based chromophores due to their low-lying ^{3}MLCT.[5h] We have designed an osmium metalloguest $[Os(biptpy)(tpy)][PF_6]_2$ bearing a biphenyl tail to bind to the cyclodextrin cavity. The $[Os(biptpy)(tpy)]^{2+}$ is luminescent at room temperature with an emission band maximum at 730 nm in 10% CH_3CN/water.

Transient absorption spectra of the separate chromophores $[Ru(ttp)(\beta\text{-CD}-ttp)][PF_6]_2$ and $[Os(biptpy)(tpy)][PF_6]_2$ in 10% CH_3CN/water are shown in Figure 4. Clearly the spectra of both systems are characterized by a relatively strong MLCT absorption and extensive ground state bleaching, around 490 nm. Maxima are observed at 380, 595, and 750 (sh) nm for the ruthenium complex and at 378, 417, 580, and 760 nm for the osmium species. Lifetimes of the excited states are ca. 1.9 ns for the $[Ru(ttp)(ttp\text{-}\beta\text{-}CD)]^{2+}$ and 100 ns for the $[Os(biptpy)(tpy)]^{2+}$ (in the presence of oxygen). Well-resolved spectra of the MLCT states of these types of compounds have not been reported before.[38]

Quinone Guest Quenching. We investigated the effect of quinones as redox-active guests on the luminescence properties of the ruthenium cyclodextrins (Scheme 2).

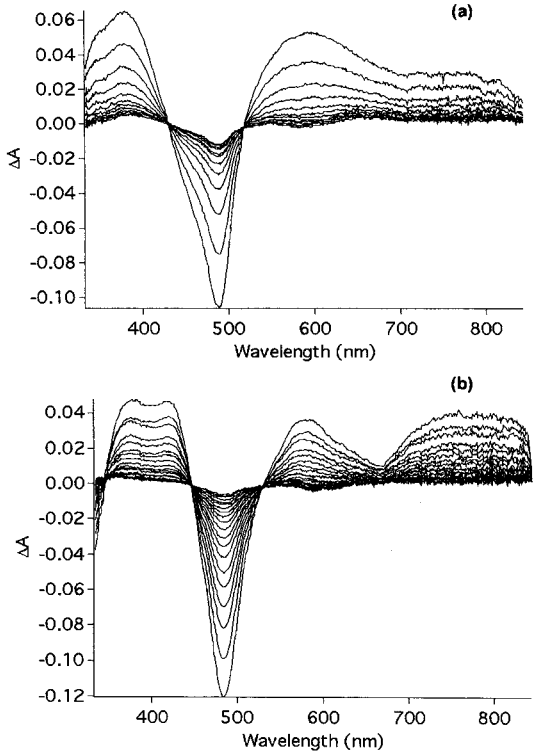

Figure 4. Representative transient absorption spectra of $[Ru(ttp)(ttp\text{-}\beta\text{-}CD)]^{2+}$ (a) and $[Os(biptpy)(tpy)]^{2+}$ (b). Conditions for $[Ru(ttp)(ttp\text{-}\beta\text{-}CD)]^{2+}$: incremental time delay 1 ns; 500 accumulations; 30 frames; $\lambda_{exc} = 450$ nm; $A(\lambda_{exc}) = 0.4$. Conditions for $[Os(biptpy)(tpy)]^{2+}$: incremental time delay 20 ns; 500 accumulations; 20 frames; $\lambda_{exc} = 450$ nm; $A(\lambda_{exc}) = 0.25$.

Quinones are popular electron acceptors for photoinduced reduction processes, involved in many examples in supramolecular assemblies.[39] Their molecular recognition properties based on hydrophobic interactions with the cyclodextrin cavity are well established.[40]

Preliminary results in our group showed quenching of the ruthenium luminescence in $[Ru(ttp)(ttp\text{-}\beta\text{-}CD)]^{2+}$ by addition of AQC indicating an electron transfer process.[16(c)] We have now carried out further studies to optimize the conditions by using different quinones and therefore varying the properties of the cyclodextrin binding as well as the redox properties of the guest. We have chosen AQC, AQS, and BQ due to their suitable redox potentials and their enhanced water solubility compared to those of other quinones. The luminescence spectra of a typical quenching experiment are shown in Figure 5.

The experiments were carried out in buffered aqueous solutions instead of water/acetonitrile to obtain better binding due to the increased ionic strength of the solution. Upon irradiation at the ruthenium ^{1}MLCT band at 490 nm, the ruthenium emission intensity at 640 nm decreases with increasing concentration of the quinone acceptor. Addition of microliter aliquots of AQS, AQC, and BQ to a solution of $[Ru(ttp)(ttp\text{-}\beta\text{-}CD)][PF_6]_2$ leads to 40%, 20%, and 25% quenching of the ruthenium ^{3}MLCT emission, respectively (Figure 6).

Excited state lifetimes of the quenched component could not be determined since the strong absorption of the quinones at the excitation wavelength used for the time-resolved emission

(36) Sauvage, J. P.; Collin, J. P.; Chambron, J. C.; Guillerez, S.; Coudret, C.; Balzani, V.; Barigelletti, F.; Decola, L.; Flamigni, L. *Chem. Rev.* **1994**, *94*, 993−1019.
(37) An artifact on the shape of the luminescence signal was previously observed although the reported[16c] λ_{max} were correct.
(38) Winkler, J. R.; Netzel, T. L.; Creutz, C.; Sutin, N. *J. Am. Chem. Soc.* **1987**, *109*, 2381.
(39) (a) Arimura, T.; Brown, C. T.; Springs, S. L.; Sessler, J. L. *Chem. Commun.* **1996**, 2293−2294. (b) Kuroda, Y.; Ito, M.; Sera, T.; Ogoshi, H. *J. Am. Chem. Soc.* **1993**, *115*, 7003−7004.
(40) Adar, E.; Degani, Y.; Goren, Z.; Willner, I. *J. Am. Chem. Soc.* **1986**, *108*, 4696−4700.

Scheme 2

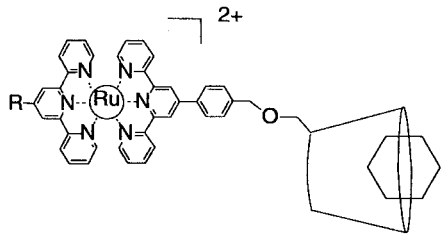

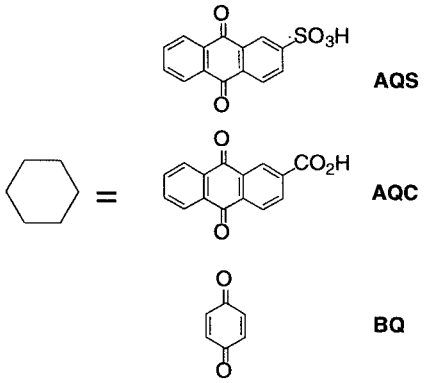

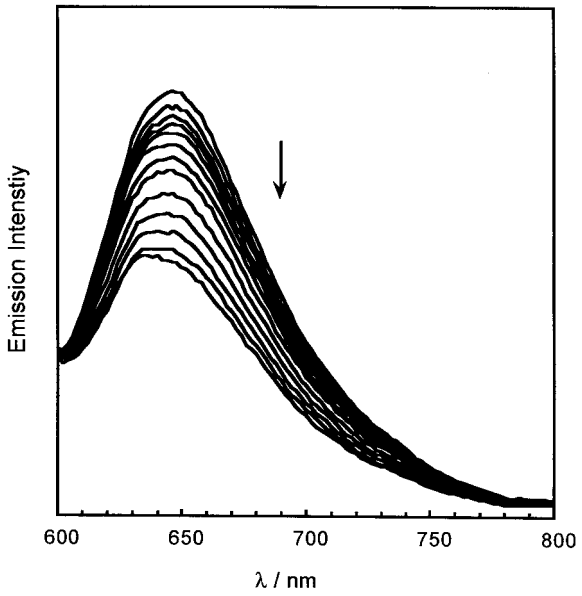

Figure 5. Luminescence spectra of $[Ru(ttp)(ttp\text{-}\beta\text{-}CD)][PF_6]_2$ (2.8×10^{-5} M) in a typical quinone quenching experiment in buffer (pH = 7). Addition of 2−62 molar equiv of AQS.

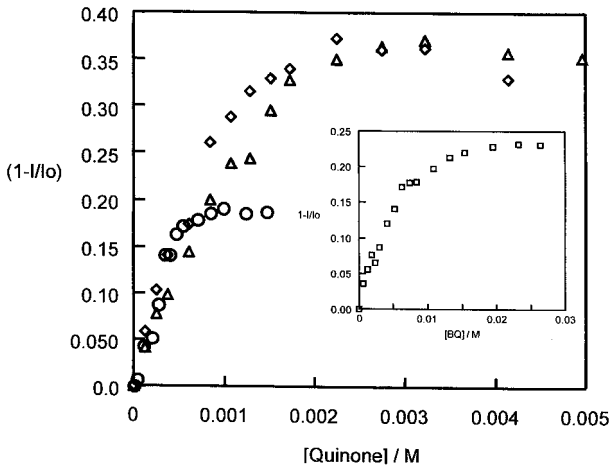

Figure 6. Stern Volmer plots of the luminescence quenching of $[Ru(ttp)(ttp\text{-}\beta\text{-}CD)]^{2+}$ and $[Ru(ttp\text{-}\beta\text{-}CD_2)]^{2+}$ by quinones. $[Ru(ttp)(ttp\text{-}\beta\text{-}CD)]^{2+}$ and AQS (◇), $[Ru(ttp)(ttp\text{-}\beta\text{-}CD)]^{2+}$ and AQC (○), $[Ru(ttp)(ttp\text{-}\beta\text{-}CD)]^{2+}$and BQ (□), and $[Ru(ttp\text{-}\beta\text{-}CD_2)]^{2+}$ and AQS (△).

(324 nm) results in strong interfering emission. An estimate of the photoinduced electron transfer rate can be obtained by using emission intensities: $k_{et} = (I_0/I - 1)/\tau_0$. Correcting for the amount of uncomplexed species results in rates of the electron transfer process of 5×10^8 and 3×10^8 s^{-1} for respectively AQS and AQC.

Control experiments using $[Ru(ttp)_2][PF_6]_2$ and quinones under the same conditions show no effect on the ruthenium luminescence, excluding any bimolecular contribution to the quenching. The assembly of the photoactive pair via the cyclodextrin cavity is necessary for the quenching to be observed. In saturation conditions, 85% for AQS and 77% for AQC are bound ($K_{AQC} = 860 \pm 200$ M^{-1}, and $K_{AQS} = 1100 \pm 100$ M^{-1}). The luminescence quenching may be attributed to an intercomponent electron transfer from the appended ruthenium center to the quinone guest inside the cavity. The driving force for the quenching of the MLCT emission depends on the reduction potential of the quinone, the oxidation potential of Ru(II)/(III), and the excited state energy of ruthenium. In our case, comparison of the quinone redox potential is satisfactory to give an indication of the relevant $\Delta G°$ since the same donor (ruthenium center) is employed. The $E_{1/2}$ values of the quinones[41] are −0.74, −0.68, and −0.51 V for AQC, AQS, and BQ, suggesting a higher driving force for BQ than AQS than AQC. Although estimates of the $\Delta G°$ values can be calculated by using

$$\Delta G = e[E_{ox} - E_{red}] - E_{00}$$

large errors are involved by the nature of the solvents employed and the measurement of redox potentials. The AQS binding is similar to the AQC binding, and the strongest quenching is attributed to the more favorable driving force. However, the weak binding of the BQ in the cyclodextrin cavity is responsible for the smaller quenching effect influencing distance and orientation factors. Although the quenching effect is not as pronounced as in the case of the ruthenium tris-bipyridine complex with an anthraquinone[42] attached at the back of one of the bipyridines, it is a considerable effect for a noncovalent intercomponent interaction between the two units. When the ruthenium bis-cyclodextrin complex, $[Ru(\beta\text{-}CD{-}ttp)_2][PF_6]_2$, was used under similar conditions, a shallower slope in the quenching was observed (Figure 6) which may be attributed to the presence of more cyclodextrin available inclusion sites.

Transient absorption spectroscopy was employed to examine the formation of the radical anion of the quinone as the transient species upon photoinduced electron transfer from $[Ru(ttp)(\beta\text{-}CD{-}ttp)]^*$ to the quinone. The transient differential absorptions upon nanosecond laser flash excitation at 459 nm of plain [Ru-

(41) (a) Meites L.; Zuman, P. *Handbook of Organic Electrochemistry*; CRC Press: Boca Raton, FL, 1976. (b) Bredereck, K.; Sommermann, F.; Diamantoglou, M. *Chem. Ber.* **1969**, *102*, 1053−1070.
(42) Oppermann, K. A.; Mecklenburg, S. L.; Meyer, T. J. *Inorg. Chem.* **1994**, *33*, 5295−5301.

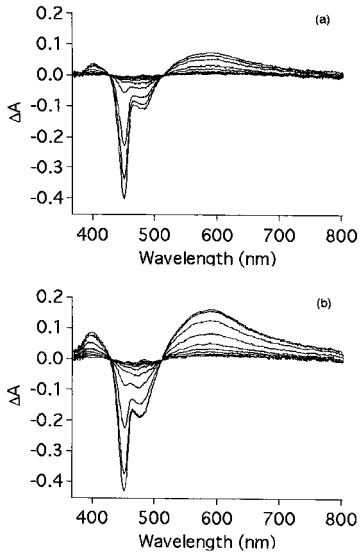

Figure 7. Transient absorption spectra of [Ru(ttp)(ttp-β-CD)]$^{2+}$ (1.26×10^{-4} M) in the presence (a) and in the absence (b) of 17 equiv of AQS: incremental time delay 1 ns; 200 accumulations; 10 frames, laser energy 1.8 mJ/pulse, $\lambda_{exc} = 450$ nm. The laser pulse at 450 nm is clearly visible as a negative signal.

(ttp)(β-CD−ttp)]$^{2+}$ and in the presence of excess AQS are shown in Figure 7.

The transient differential absorption spectrum of [Ru(ttp)(β-CD−ttp)]$^{2+}$ shows bleaching of the ground state absorption band at 490 nm, in addition to new strong absorption bands at both higher (600 nm) and lower (400 nm) wavelengths. The broad band centered at 600 nm is attributed to the ttp$^{\bullet-}$ in accordance with previous studies in ruthenium complexes.[43] The anthraquinone radical anion is expected to absorb at 590 nm,[44] which falls in the same area as the absorption of ttp$^{\bullet-}$. Upon addition of excess of AQS no apparent changes were observed in the general features of the [Ru(ttp)(β-CD−ttp)]$^{2+}$ transient spectrum, besides an overall decrease of the MLCT state absorption. The overall decrease is in accordance with the steady state emission quenching. About 40% of the MLCT state is quenched. As an alternative method, the decay of the 600 nm band which indicated the recovery of the ground state was monitored. A decay with lifetime of $\tau = 1.9$ ns was measured, characteristic of the ruthenium species. The spectra are dominated by ttp$^{\bullet-}$ absorption, which might be due to very fast back electron transfer. A similar problem was observed in the case of a ruthenium complex where the anthraquinone unit was attached covalently to the ligand.[42] Experimental limitations with the excitation wavelength of the single photon counting setup made it impossible to determine the emission lifetime decrease due to the strong emission of the quinone upon 324 nm excitation.

Osmium Metalloguest Communication. The photoinduced communication between the two metal centers, ruthenium and osmium, assembled by the cyclodextrin cavity can be established either by energy transfer due to the lower-lying ^{3}MLCT state of osmium or by electron transfer from the ruthenium excited state to an Os(III) species.

The energy transfer from the ruthenium-appended cyclodextrin [Ru(ttp)(β-CD−ttp)][PF_6]$_2$ to the osmium(II) guest has been examined in aqueous solutions using steady state and time-resolved luminescence experiments. To demonstrate energy transfer from the Ru(II) to the Os(II) by steady state luminescence spectroscopy, sensitization of the osmium luminescence or quenching of the ruthenium emission is expected upon excitation to the ruthenium center. Due to the fact that these two chromophores have very close ^{1}MLCT energy levels, selective excitation on the ruthenium band is not possible. Therefore, the procedure described by Barigelletti et al.[45] using isoabsorptive solutions has been followed. In our case an excess of the [Ru(ttp)(β-CD−ttp)]$^{2+}$ was required to ensure inclusion of most of the osmium guest molecules (up to 63%, $K = 2 \times 10^4$ M^{-1})[27] inside the ruthenium−cyclodextrin cavity. Different ratios of [Os(biptpy)(tpy)]$^{2+}$/[Ru(ttp)(β-CD−ttp)]$^{2+}$ were examined for sensitization of the osmium emission. However, no sensitization could be observed within the experimental error of the experiment. The decay of the ruthenium emission was also monitored by addition of an excess of the osmium guest. Even though a short component was observed when a ratio of 8:1 was employed (80% of the guest was bound), it was only a small percentage of the signal (10%) and its assignment is ubiquitous due to the limitations of the accuracy of the experiment. The inefficiency of the energy transfer between terpyridine-based ruthenium/osmium conjugates has been previously observed via saturated spacers[46] between the two chromophore units and has been attributed to the short-lived luminescence of the donor and a relatively small driving force.

The noncovalent communication between the ruthenium−cyclodextrin compounds and an osmium metalloguest was also studied by making use of the well-known chemical oxidation of the Os(II) to Os(III) and studying the ruthenium(II) to osmium(III) photoinduced electron transfer (Scheme 3). The Os(III) species, generated by using cerium(IV) as an oxidizing agent,[47,48] is a good electron acceptor that can quench the ruthenium-based MLCT luminescence ($\Delta G^\circ \approx -1.6$ eV).[34]

The lifetime of Ru(II) is quenched by the presence of 7 molar equiv of Os(III) metalloguest. The time-resolved luminescence experiment results, Figure 8, show that the unquenched ruthenium has a lifetime of 1.9 ns; in the presence of Os(III) deconvolution of the lifetime decay reveals a component of 100 ± 10 ps (80%) and a component of 1.9 ns (20%). The fast component is attributed to electron transfer from Ru(II) to Os(III) giving an electron transfer rate 9.5×10^9 s^{-1}. Whereas the addition of [Os(biptpy)(tpy)][PF_6]$_2$ or $(NH_4)_4Ce(SO_4)_4$ does not change the luminescence lifetime of [Ru(ttp)(ttp-β-CD)][PF_6]$_2$, its lifetime is strongly reduced in the presence of both components.

Independent binding studies of the guest to the cyclodextrin demonstrate that in the same conditions 80% of the osmium guest is bound. This indicates the high efficiency of the photoinduced electron transfer process as expected of the high ΔG°.

(43) Collin, J.-P.; Harriman, A.; Heitz, V.; Odobel, F.; Sauvage, J.-P. *J. Am. Chem. Soc.* **1994**, *116*, 5679−5690.
(44) Fujita, M.; Ishida, A.; Majima, T.; Takamuku, S. *J. Phys. Chem.* **1996**, *100*, 5382−5387.
(45) Barigelletti, F.; Flamigni, L.; Balzani, V.; Collin, J.-P.; Sauvage, J.-P.; Sour, A.; Constable, E. C.; Cargill Thompson, A. M. W. *J. Am. Chem. Soc.* **1994**, *116*, 7692−7699.
(46) (a) Sauvage, J.-P. Hammarström, L.; Barigelletti, F.; Flamigni, L.; Armaroli, N.; Sour, A.; Collin, J.-P. *J. Am. Chem. Soc.* **1996**, *118*, 11972−11973. (b) Barigelletti, F.; Flamigni, L.; Balzani, V.; Collin, J.-P.; Sauvage, J.-P.; Sour, A. *New J. Chem.* **1995**, *19*, 793−798.
(47) De Cola, L.; Balzani, V.; Barigelletti, F.; Flamigni, L.; Belser, P.; Von Zelewsky, A.; Frank, M.; Vogtle, F. *Inorg. Chem.* **1993**, *32*, 5228−5238.
(48) Bilakhiya, A. K.; Tyagi, B.; Paul, P. *Polyhedron* **2000**, *19*, 1233−1243.

Scheme 3

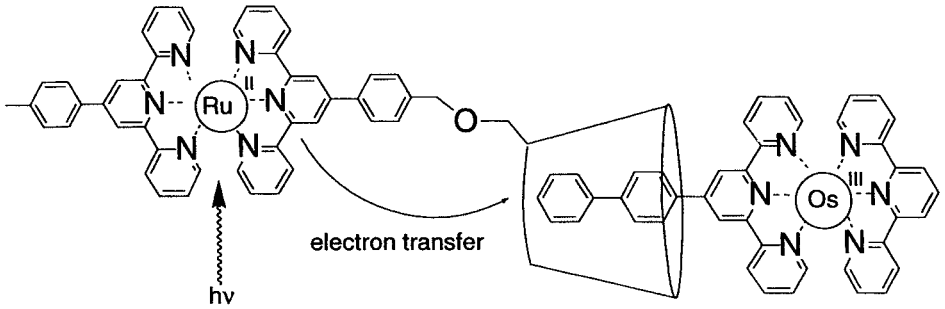

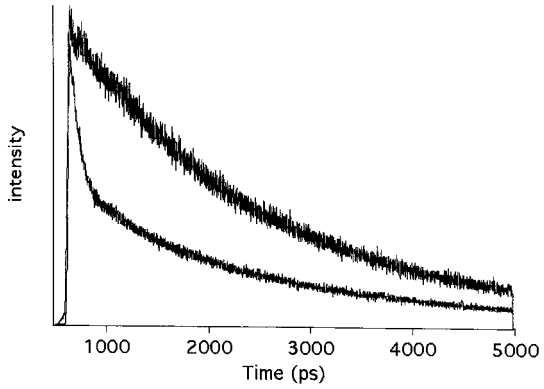

Figure 8. Time-resolved emission of $[Ru(ttp)(ttp\text{-}\beta\text{-}CD)]^{2+}$ in 10% CH_3CN/water in the absence and in the presence (signal with short component) of 7 equiv of $[Os(biptpy)(tpy)]^{3+}$ metalloguest ($\lambda_{exc} = 324$ nm).

Measurements of $[Ru(ttp)_2]^{2+}$ under identical conditions do not show quenching of the ruthenium lifetime. In the $[Ru(ttp)(ttp\text{-}\beta\text{-}CD)][PF_6]_2$ system, the photoinduced electron transfer is mediated by supramolecular cyclodextrin complexation: a photoinduced intercomponent process.

Conclusions

Photoactive ruthenium−cyclodextrins have been shown to be versatile building blocks for the design of supramolecular assemblies encompassing donor/acceptor units. Quenching of the ruthenium luminescence by quinone guests is observed indicating an intramolecular process via the cyclodextrin cavity, which is optimized when AQS is used as the electron acceptor guest. Metalloguests have also been assembled with the ruthenium cyclodextrins to study the communication between the metal centers. Electron transfer from the ruthenium(II) center appended to the cyclodextrin to an osmium(III) metalloguest in the cyclodextrin cavity has been observed. The photoinduced process between the two metal centers is established via noncovalent bonds in aqueous solutions.

Acknowledgment. We are grateful to EPSRC (J.M.H. GR/L91788) and Leverhulme Trust (M.C.) for financial support and the British Council for a travel exchange grant. We also wish to thank Johnson & Matthey for a loan of ruthenium trichloride and American Maize Products for providing a gift of cyclodextrin. We thank Mara Staffilani, Anouk Dirksen, and Mattijs Koeberg for their contributions to this work.

IC0100166